

This is the peer reviewed version of the following article: Ni, P, Li, J, Hao, H, et al. Time-varying system identification using variational mode decomposition. Struct Control Health Monit. 2018; 25(6):e2175, which has been published in final form at <https://doi.org/10.1002/stc.2175>. This article may be used for non-commercial purposes in accordance with Wiley Terms and Conditions for Use of Self-Archived Versions. This article may not be enhanced, enriched or otherwise transformed into a derivative work, without express permission from Wiley or by statutory rights under applicable legislation. Copyright notices must not be removed, obscured or modified. The article must be linked to Wiley's version of record on Wiley Online Library and any embedding, framing or otherwise making available the article or pages thereof by third parties from platforms, services and websites other than Wiley Online Library must be prohibited.

## Time-varying System Identification using Variational Mode Decomposition

Pinghe Ni<sup>1, 2</sup>, Jun Li<sup>1, \*</sup>, Hong Hao<sup>1</sup>, Yong Xia<sup>2</sup>, Xiangyu Wang<sup>3</sup>,  
Jae-Myung Lee<sup>4</sup>, Kwang-Hyo Jung<sup>4</sup>

<sup>1</sup>*Centre for Infrastructural Monitoring and Protection, School of Civil and Mechanical Engineering, Curtin University, Kent Street, Bentley, WA 6102, Australia*

<sup>2</sup>*Department of Civil and Environmental Engineering, The Hong Kong Polytechnic University, Hung Hom, Kowloon, Hong Kong*

<sup>3</sup>*Australasian Joint Research Centre for Building Information Modelling, School of Built Environment, Curtin University, Perth, WA 6845, Australia*

<sup>4</sup>*Department of Naval Architecture and Ocean Engineering, Pusan National University, Busan, Korea*

**Abstract:** This paper proposes a new time-varying system identification approach based on variational mode decomposition (VMD), which decomposes the measured responses as a finite number of Intrinsic Mode Functions (IMFs). The instantaneous frequencies of time-varying systems are identified by performing the Hilbert transform of each decomposed IMF. The effectiveness of the proposed approach is verified through numerical studies on a time-varying system under an impact force. Experimental validations on analyzing the measured vibration data in the laboratory from a steel frame structure and a time-varying bridge-vehicle system are conducted. The identified instantaneous modal frequencies by the presented technique are compared with those using Empirical Mode Decomposition (EMD) based methods. The results demonstrate that the proposed approach can identify the instantaneous frequencies of time-varying systems with a better accuracy.

**Keywords:** Modal identification; Time-varying systems; Variational mode decomposition (VMD); Instantaneous frequency; Bridge-vehicle system

\*Corresponding Author, Centre for Infrastructural Monitoring and Protection, School of Civil and Mechanical Engineering, Curtin University, Kent Street, Bentley, WA 6102, Australia.  
Email: [junli@curtin.edu.au](mailto:junli@curtin.edu.au); [LI.Jun@connect.polyu.hk](mailto:LI.Jun@connect.polyu.hk), Tel.: +61 8 9266 5140; Fax: +61 8 9266 2681.

# 1 Introduction

Modal identification is ~~anone~~ of important fields in structural dynamics and health monitoring. Over the past several decades, modal identification has gained significant attentions and numerous methods have been developed [1], which help us to extract the vibration characteristics of structures and better understand their vibration behaviors. Since most of structures are under ambient excitations, methods like frequency domain decomposition (FDD) method [2], time domain decomposition method [3], stochastic subspace identification (SSI) method [4] are more promising for civil engineering structures. These methods are proposed for structure based on the assumption of ~~under~~ white noise excitations. Eigensystem Realization Algorithm (ERA) method [5] are proposed for modal identification with free-vibration response. To improve the ERA method and make it possible for modal identification ~~offer~~ structures under environmental excitation, Natural Excitation Technique [6] and Random Decrement Technique [7] are proposed. It is proved that the correlation functions/random decrement functions have the same properties as free vibration responses. The measured ~~ement~~ vibration signal usually contains noise. Dohler et al. [8] extended SSI method and the uncertainty bounds in the modal identification results can be quantified. Bayesian based approaches [9-12] are another widely used methods for modal identification, considering the measurement noise effect. Bayesian based approaches have been successfully ~~applied~~ used in identification of vibration properties of real structures [13-15].

Those above-mentioned methods have been proposed for the modal identification of time-invariant systems. However, the dynamic characteristics of civil engineering structures often change over time during their service life. For example, natural frequencies of long span bridges may vary due to the environmental effects, i.e. temperature and humidity [16, 17]. Other examples include the bridge-vehicle system when a number of vehicles or a heavy train crosses a bridge and the bridge cable with stiffness changing with the tension force [18]. In these cases, the bridge-vehicle system is time-varying with the changing locations of the moving vehicle on the bridge. It is essential to understand and identify the time-varying dynamic characteristics such as instantaneous modal frequencies, which can be very useful for monitoring the structural operational condition and identifying possible damage in the structure.

Studies on time-varying system identification have been conducted. Bao et al. [19] proposed an adaptive time-frequency analysis method for the identification of time-varying cable tension forces. A functional series vector time-dependent autoregressive moving average method was proposed to identify the time-varying frequencies of a bridge-vehicle system in the laboratory [20]. Empirical Mode Decomposition (EMD), which was developed by Huang et al. [21], has attracted significant attention for vibration signal decomposition. EMD decomposes a specific signal into a finite number of IMFs. Instantaneous frequencies are then identified by performing Hilbert-Huang Transform (HHT) with extracted IMFs. Shi et al. [22] used the complete measurement responses to identify the time-varying properties of linear systems. Yang and Chang [23] developed a method to extract the bridge frequencies from the dynamic response of a passing vehicle by using EMD. Both theoretical and experimental investigations demonstrated that higher modes of vehicle-bridge system can be identified through preprocessing of the data by the EMD technique. Li et al. [24] proposed a combination method to detect the changes in structural responses by using EMD and wavelet analysis. This technique was capable of identifying the time and extent of the damage more precisely through the magnitude of the wavelet coefficient of the dominant IMF than using the individual wavelet transform of the original response signal. Li and Hao [25] used EMD and HHT to identify the damage of shear connectors in composite bridges under moving loads with the measured relative displacements.

A variety of alternative methods have been further developed for signal decomposition. Feldman [26] developed an iterative signal decomposition method, referred as time-varying vibration decomposition. Chen and Wang [27] proposed an Analytical Mode Decomposition (AMD) method for analyzing the narrowband time series with closely spaced frequency components. Results showed that AMD can accurately decompose a time series into two components with Fourier spectra non-vanishing over two mutually exclusive frequency ranges separated by a constant bisecting frequency. The instantaneous frequency of time-varying and time-invariant systems can be accurately evaluated by AMD-Hilbert spectrum analysis [28, 29]. A method based on continuous wavelet transform was proposed for the instantaneous frequency identification of time-varying structures [30]. The instantaneous frequencies were identified from the extracted wavelet ridges, and a penalty function was proposed to reduce the noise

effect. The accuracy of the method was verified with experimental studies on a cable with time-varying tension force. A wavelet-based Frequency Response Function (FRF) was proposed by Staszewski and Wallace [31]. It was represented in the time–frequency domain, and time averaging was performed to improve the signal-to-noise ratio. The proposed method was successfully applied to identify the time-varying frequency of a bridge-vehicle system.

Variational Mode Decomposition (VMD) is a recently proposed novel technique for adaptive signal decomposition [32]. It is demonstrated that VMD is effective in decomposing a signal into an ensemble of band-limited IMFs. To the authors' best knowledge, there has been no study yet on using this relatively new technique for the instantaneous frequency identification of time-varying systems. This paper applied this newly developed VMD technique to perform the signal decomposition and identify the instantaneous frequencies of time-varying systems. It decomposes the measured response as a finite number of IMFs. Each mode is an amplitude-modulated-frequency-modulated (AMFM) signal with the narrow-band property and nonnegative smoothly varying instantaneous frequencies. The instantaneous frequencies of time-varying systems are identified by performing the Hilbert transform of decomposed IMFs. Numerical studies on analysing the response of a time-varying system under an impact force are conducted to demonstrate the effectiveness and performance of the proposed approach in the instantaneous frequency identification. Experimental studies on analyzing the measured vibration data in the laboratory from a steel frame structure and a time-varying bridge-vehicle system are conducted. The comparison between the results from the proposed approach and an existing method demonstrates the advantage of the proposed approach.

## 2 Theoretical background

### 2.1 Modal response of time-varying structures

The equation of motion of a  $n$  DOF time-varying structure can be expressed as

$$\mathbf{M}(t)\ddot{\mathbf{x}}(t) + \mathbf{C}(t)\dot{\mathbf{x}}(t) + \mathbf{K}(t)\mathbf{x}(t) = \mathbf{F}(t) \quad (1)$$

where  $\mathbf{M}(t)$ ,  $\mathbf{C}(t)$  and  $\mathbf{K}(t)$  are  $n \times n$  time-varying mass, damping and stiffness matrices, respectively;  $\mathbf{x}(t) = [x_1(t), x_2(t), \dots, x_n(t)]^T$  is the displacement response vector,  $\dot{\mathbf{x}}(t)$  and

$\dot{\mathbf{x}}(t)$  are the velocity and acceleration response vectors, respectively;  $\mathbf{F}(t)$  is the excitation force vector on the structure. In this study, the mass and damping matrices are assumed as time invariant as their variations are usually less significant as compared with that of the structural stiffness.

When the time variation of the coefficient is small, the frequency of each mode (variation of each mode) is narrow-band. Structural displacement and acceleration responses can be obtained as the superposition of  $n$  vibration modal responses. Based on the modal superposition principle [30], the signal can be written as

$$\mathbf{x}(t) = \sum_{i=1}^n \Phi_i(t) q_i(t), \quad \ddot{\mathbf{x}}(t) = \sum_{i=1}^n \Phi_i(t) \ddot{q}_i(t) \quad (2)$$

where  $\Phi_i(t)$  is the  $i$ -th modal shape vector, and  $q_i(t)$  is the associated generalized modal coordinate. Substituting Eq. (2) into Eq. (1) and using the orthogonal properties of the mode shapes, Eq. (1) can be decoupled into equations of  $n$  modes

$$\ddot{q}_i(t) + 2\xi_i\omega_i(t)\dot{q}_i(t) + \omega_i^2 q_i(t) = \Phi_i^T(t) \mathbf{F}(t) / m_i \quad (3)$$

where  $\omega_i(t)$ ,  $\xi_i(t)$  and  $m_i$  denote the  $i$ -th modal frequency, modal damping ratio and modal mass, respectively.

When an impulse force is applied on the  $z$ -th DOF, the acceleration response of the  $i$ -th generalized modal coordinate is given as

$$\ddot{q}_i(t) = \frac{F_0 \phi_{zi,t=0} \omega_i(t)}{m_j \sqrt{1 - \xi_i^2}} e^{-\xi_i \omega_i(t)} \cos(\omega_{di}(t)t + \nu_i) \quad (4)$$

where  $\phi_{zi,t=0}$  is the  $z$ -th item of the  $i$ -th modal vector  $\Phi_i(t)$  at time  $t=0$ ,  $\omega_{di}(t) = \omega_i(t) \sqrt{1 - \xi_i^2}$ , and  $\nu_i$  is the phase angle.

The acceleration response  $\ddot{x}_p(t)$  of the structure at the  $p$ -th DOF is given as

$$\ddot{x}_p(t) = \sum_{i=1}^n \phi_{pi}(t) \ddot{q}_i(t) \quad (5)$$

It can be further written as the superposition of AMFM signals

$$\ddot{x}_p(t) = \sum_{i=1}^n u_i = \sum_{i=1}^n A_i(t) \cos(\omega_{di}(t)t + \nu_i) \quad \text{and} \quad A_i(t) = \frac{\phi_{pi}(t) F_0 \phi_{zi,t=0} \omega_i(t)}{m_j \sqrt{1 - \xi_i^2}} e^{-\xi_i \omega_i(t)} \quad (6)$$

## 2.2 Variational mode decomposition

VMD can be used to decompose a signal into a discrete number of IMFs with the specific sparsity properties of its bandwidth in the spectral-frequency domain and each mode is compact around a center frequency. A core assumption of VMD is the limited bandwidth of the individual modes.

An IMF  $u_k(t)$  is defined as an AMFM signal, which is expressed as

$$u_k(t) = A_k(t) \cos(\varphi_k(t)) \quad (7)$$

where  $\varphi_k(t)$  and  $A_k(t)$  denote the phase and the envelope of the  $k$ -th IMF, respectively; and the instantaneous frequency  $\omega^k(t) = \partial \varphi_k(t) / \partial t$  is nonnegative and vary much slower than the phase  $\varphi_k(t)$ .

The detailed description of VMD method can be found in [32-34]. The current signal decomposition methods are limited by: 1) The algorithms lack mathematical theory, i.e. EMD; 2) The vulnerability to noise effect and 3) The hard band-limits of wavelet approaches [32]. VMD is to decompose the measured acceleration signal  $\ddot{x}_p(t)$  into a discrete number of modes that have specific sparsity properties while reproducing the input. The process can be expressed as a constrained variational problem with the following equation [32]

$$\min_{\{u_k\}, \{\bar{\omega}_k\}} \left\{ \sum_{k=1}^K \left\| \partial_t \left[ \left( \delta(t) + \frac{j}{\pi t} \right) * u_k(t) \right] e^{-j\bar{\omega}_k t} \right\|_2^2 \right\}, \text{ subjected to } \sum_{k=1}^K u_k(t) = \ddot{x}_p(t) \quad (8)$$

where  $\delta$  is the Dirac function,  $*$  denotes the convolution,  $\{u_k\} = \{u_1, u_2, \dots, u_K\}$  and  $\{\bar{\omega}_k\} = \{\bar{\omega}_1, \bar{\omega}_2, \dots, \bar{\omega}_K\}$  are shorthand notations for the set of all modes and their center frequencies, respectively.

Using a quadratic penalty term and Lagrangian multipliers  $\lambda$ , the above constrained variational problem can be transferred into an unconstrained optimization problem as

$$L(\{u_k\}, \{\bar{\omega}_k\}, \lambda) = \alpha \sum_{k=1}^K \left\| \partial_t \left[ \left( \delta(t) + \frac{j}{\pi t} \right) * u_k(t) \right] e^{-j\bar{\omega}_k t} \right\|_2^2 + \left\| \sum_{k=1}^K u_k(t) - \ddot{x}_p(t) \right\|_2^2 + \left\langle \lambda(t), \ddot{x}_p(t) - \sum_{k=1}^K u_k(t) \right\rangle \quad (9)$$

where the regularization parameter  $\alpha$  depends on the data fidelity constraint. The quadratic penalty term is considered due to the noise effect, while Lagrangian multipliers are a common way of enforcing constraints. These two terms are used to improve the convergence properties and the strict enforcement of the constraints [32].

The solution of minimizing Eq. (9) can be obtained through a sequence of iterative sub-optimizations called the alternate direction method of multipliers (ADMM) [35], which is used to find out the different decomposed modes and center frequencies. Each mode can be represented as

$$u_k(\omega) = \frac{\ddot{x}_p(\omega) - \sum_{i \neq k} u_i(\omega) + (\lambda(\omega)/2)}{1 + 2\alpha(\omega - \bar{\omega}_k)^2} \quad (k=1, 2, \dots, K) \quad (10)$$

where  $\ddot{x}_p(\omega)$  is the Fast Fourier transform of the signal  $\ddot{x}_p(t)$ .

VMD mainly consists of following steps:

*Step 1: Intrinsic mode update.* The mode  $u_k^{n+1}(\omega)$  is updated with Eqs. (11a) and (11b). The Wiener filtering is embedded for updating the mode directly in Fourier domain with a filter tuned to the current center frequency  $\bar{\omega}_k^n$ .

$$u_k^{n+1}(\omega) = \frac{\ddot{x}_p(\omega) - \sum_{i < k} u_i^{n+1}(\omega) - \sum_{i > k} u_i^n(\omega) + (\lambda^n(\omega)/2)}{1 + 2\alpha(\omega - \bar{\omega}_k^n)^2} \quad (k=1, 2, \dots, K) \quad (11a)$$

$$u_k^{n+1}(t) = \Re \{ \text{ifft} (u_k^{n+1}(\omega)) \} \quad (11b)$$

where  $\text{ifft}(\cdot)$  is the inverse Fast Fourier transform of a signal and  $\Re\{\cdot\}$  denotes the real part of an analytic signal.

*Step 2: Center frequency update.* The center frequency  $\bar{\omega}_k^{n+1}$  is updated as the center of gravity of the corresponding mode's power spectrum as

$$\bar{\omega}_k^{n+1} = \frac{\int_0^\infty \omega |u_k^{n+1}(\omega)|^2 d\omega}{\int_0^\infty |u_k^{n+1}(\omega)| d\omega} \quad (k=1, 2, \dots, K) \quad (12)$$

*Step 3: Dual ascent-update.* For all frequencies  $\omega \geq 0$ , the Lagrangian multiplier  $\lambda^{n+1}(\omega)$  is updated by Eq. (13) as dual ascent to enforce the exact signal reconstruction until the convergence criteria as shown in Eq. (14) is satisfied.

$$\lambda^{n+1}(\omega) = \lambda^n(\omega) + \tau \left( \ddot{x}_p(\omega) - \sum_k u_k^{n+1} \right) \quad (13)$$

$$\sum_{k=1}^K \frac{\|u_k^{n+1} - u_k^n\|_2^2}{\|u_k^n\|_2^2} \leq \varepsilon \quad (14)$$

### 2.3 Hilbert transform

After performing the signal decomposition with VMD, each IMF can be obtained and used for calculating the Hilbert spectrum. The Hilbert transform of the  $k$ -th IMF  $u_k(t)$  can be expressed as

$$\tilde{u}_k(t) = H[u_k(t)] = \frac{1}{\pi} P \int_{-\infty}^{+\infty} \frac{u_k(\tau)}{t - \tau} d\tau \quad (15)$$

where  $P$  represents the Cauchy principle value and  $\tilde{u}_k(t)$  is the Hilbert transform of  $u_k(t)$ .

With IMF and the Hilbert transform, an analytical signal can be defined as

$$z_k(t) = u_k(t) + i\tilde{u}_k(t) = A_k(t) e^{j\theta_k(t)} \quad (16)$$

$$A(t) = [u_k(t)^2 + \tilde{u}_k(t)^2]^{1/2} \quad (17)$$

$$\theta_k(t) = \arctan \left( \frac{\tilde{u}_k(t)}{u_k(t)} \right) \quad (18)$$

Finally, the identified instantaneous frequency  $\omega_{id}^k(t)$  of  $k$ -th component can be obtained as

$$\omega_{id}^k(t) = \frac{\partial \theta_k(t)}{\partial t} \quad (19)$$

To generally avoid the ambiguities due to possible phase unwrapping in Eq. (19), the



instantaneous frequency  $\omega_{id}^k(t)$  of the  $k$ -th component can be identified as

$$\omega_{id}^k(t) = \frac{u_k(t) \frac{\partial \tilde{u}_k(t)}{\partial t} - \tilde{u}_k(t) \frac{\partial u_k(t)}{\partial t}}{u_k(t)^2 + \tilde{u}_k(t)^2} \quad (20)$$

### 3 Numerical studies

Numerical studies on a time-varying Multi-Degrees-of-Freedom (MDOF) shear type building structure are conducted in this section to demonstrate the effectiveness and accuracy of the proposed approach. The equation of motion of a four DOF shear type building can be described as follows

$$\begin{bmatrix} m_1 & & & \\ & m_2 & & \\ & & m_3 & \\ & & & m_4 \end{bmatrix} \begin{bmatrix} \ddot{x}_1(t) \\ \ddot{x}_2(t) \\ \ddot{x}_3(t) \\ \ddot{x}_4(t) \end{bmatrix} + \begin{bmatrix} c_1+c_2 & -c_2 & & \\ -c_2 & c_2+c_3 & -c_3 & \\ & -c_3 & c_3+c_4 & -c_4 \\ & & -c_4 & c_4 \end{bmatrix} \begin{bmatrix} \dot{x}_1(t) \\ \dot{x}_2(t) \\ \dot{x}_3(t) \\ \dot{x}_4(t) \end{bmatrix} + \begin{bmatrix} k_1+k_2 & -k_2 & & \\ -k_2 & k_2+k_3 & -k_3 & \\ & -k_3 & k_3+k_4 & -k_4 \\ & & -k_4 & k_4 \end{bmatrix} \begin{bmatrix} x_1(t) \\ x_2(t) \\ x_3(t) \\ x_4(t) \end{bmatrix} = \begin{bmatrix} 0 \\ 0 \\ f(t) \\ 0 \end{bmatrix} \quad (21)$$

where  $m_1=m_2=m_3=m_4=4kg$ ,  $c_1=c_2=c_3=c_4=0.5 \text{ N/(m}^{-1}\text{s)}$ ,  $k_3=k_4=1.2 \times 10^4 \text{ N/m}$ ,  $k_1$  and  $k_2$  are the time-varying stiffness parameters.

Two cases with smooth and periodical variations are studied respectively. In Case 1, the varying stiffness properties are  $k_1 = (1 - 0.04t) \times 10^4 \text{ N/s}$  and  $k_2 = (1.2 - 0.03t) \times 10^4 \text{ N/s}$ . In Case 2,  $k_1 = (1 + 0.3 \sin(2\pi t)) \times 10^4 \text{ N/s}$  and  $k_2 = 1.2 \times 10^4 \text{ N/m}$ .

The following impulse force is applied at the third floor

$$f(t) = \begin{cases} 200 \text{ N} & t=0 \\ 0 & t \neq 0 \end{cases} \quad (22)$$

The analytical responses of the time-varying system are obtained by using a typical time-stepped integration method, such as Newmark-beta method. The sample frequency is set as 200 Hz. The acceleration signal from the top level is selected for the decomposition and instantaneous frequency identification. 3% gauss white noise is added to the simulated response signals in both two cases to consider the measurement noise effect.

### 3.1 Instantaneous frequency identification

Figure 1 shows the time history and Fourier transform spectrum of the response signal from Case 1. Four clear frequencies are observed in the Fourier spectrum and therefore the number of frequency components  $K$  in Equation (10) for the signal decomposition using VMD is defined as 4. Figure 2 shows the decomposed IMFs and their frequency spectra. As shown in the Fourier spectra, those four independent frequency components are successfully decomposed and well separated. Figure 3 shows the true and identified instantaneous frequencies of the time-varying system. It is noted that the theoretical instantaneous frequency is obtained with "freezing method" [36]. The method assumes that the system is a time-invariant system in each time interval, and the theoretical instantaneous frequency in this time interval is calculated by solving an eigenvalue problem. The end effect caused by the finite length and an incomplete cycle included in a signal may bring certain errors in the identification results, especially at the beginning and end of the response signal, as observed in Figure 3. If band-pass filters are used for the signal analysis, the frequency range of the defined bands needs to be carefully selected. The end and leakage effects may be significant in the associated FFT analysis. Besides, the simply analysis by using band-pass filters is not able to identify the instantaneous frequency. However, it is noted that smooth decreasing time-varying frequencies are successfully identified with the proposed approach.

Figures 4-6 show the response signal in time and frequency domains, decomposed IMF by using VMD, and the identified instantaneous frequencies for Case 2, respectively. The Fourier spectra of the decomposed IMFs, as shown in Figure 5, indicates that the four modes are clearly decomposed without any overlapping. In the identified instantaneous frequencies as shown in Figure 6, the variation in the low frequency mode is larger than that in the high frequency modes. The identified second mode is better than other modes. The reason is that the response signal contains the largest energy in the second mode, which can be observed in Figure 4. The identified low mode frequency fluctuates around the central frequency and the high mode offsets the central frequency. This maybe because of the noise effect. A traditional signal decomposition method, i.e. EMD, is also applied to decompose the response signal of Case 2 and the obtained IMFs are given in Figure 7. Several unwanted IMFs appear. The Hilbert

transform is then applied to the first three IMFs and the identified instantaneous frequencies are shown in Figure 8. The first two modes have significant fluctuations. The third and the fourth modes are near each other, and EMD fails to decompose these two modes. The decomposition of signals calculated from time-varying systems is challenging. As observed in Figure 4, there are several peaks around the most significant frequency components in the Fourier spectrum, which makes the signal decomposition using traditional methods difficult. The performance of using EMD for signal decomposition is vulnerable to the noise in the measurements and significant fluctuations may be observed in the results, as shown in Figure 7-8. Comparing the identification results as shown in Figures 6 and 8 by using VMD and EMD respectively, VMD provides a better solution for the signal decomposition.

### 3.2 Measurement noise effect

To further investigate the robustness and performance of the proposed approach by using VMD, 5% and 10% noises are added in the response simulated in Case 2. Before using the noisy responses for the signal decomposition, since the first four are observed within 30Hz, a band-pass filter of the frequency range from 1 Hz~30 Hz is applied to the noisy responses to reduce the high frequency noise. The same procedure is followed with VMD used for signal decomposition, and the instantaneous frequencies from these noisy responses are identified as shown in Figure 9. It can be observed that all the four frequency components are successfully separated and the identified instantaneous frequencies are close to the true values. The best agreement is observed for the results on the second mode. The reason, as discussed above, is that the vibration is dominated by the second mode. The results of other modes, including modes 3 and 4, are also satisfactory under such high noise effects.

## 4 Experimental verifications

VMD can be used for the decomposition of both stationary and non-stationary signals. Existing methods may have some limitations in dealing with signals from time-invariant system owing to the, i.e. end effects. To investigate the effectiveness and performance of using the proposed approach for the instantaneous frequency identification of civil engineering structures,

experimental studies on a time-invariant structure and a time-varying structure are conducted in the laboratory. The measured vibration data are used for the signal decomposition and extracting the instantaneous frequencies of the structures with the proposed approach. Experimental studies on the first time-invariant structure are used to demonstrate the advantage and accuracy of the proposed approach over an existing method. The second example is a bridge-vehicle system, which is a time-varying structure. Experimental validations are conducted to demonstrate the applicability and efficiency of using VMD for signal decomposition and instantaneous frequency identification.

#### **4.1 Modal identification of a time-invariant structure**

The first example is a time-invariant four-story shear-type steel frame structure, as shown in Figure 10. Its dimensions are shown in Figure 11. The height and width of the model are 1200 mm and 595 mm, respectively. The cross section of the steel beams is 100 mm by 25 mm. Both columns are of 50 mm wide and 5 mm thick. The beams and columns were welded together to form rigid joints. The bottom of the two columns were welded onto a thick and solid steel plate, which was fixed to the strong floor. A SINOCERA LC-04A hammer with a rubber tip was used to excite the frame, and horizontal acceleration responses of the frame were measured at each floor with KD1300 accelerometers. A commercial data logging system INV306U and its associated signal analysis package DASP V10 were used for data acquisition and analysis. The sampling frequency was set as 1024 Hz, and the cut-off frequency range was preset as 1 Hz to 300 Hz for all test cases.

Experimental tests were performed by using the hammer to hit the top floor of the frame. The acceleration responses were recorded with a duration of 60 seconds. The measured response signals were resampled to 100 Hz, which not only removes the high-frequency measurement noise but also reduces the computational workload. The measured acceleration response at the top level of the frame structure and its Fourier spectrum are shown in Figure 12.

An improved HHT method [37] based on EMD is used to analyze the measured response at the top level for a comparison study. Band-pass filters techniques are also applied to the measured response first before the signal decomposition using EMD. Four pass bands are set as 4 Hz ~ 6 Hz, 14 Hz ~ 16 Hz, 23 Hz ~ 25 Hz, and 28 Hz ~ 30 Hz, respectively, according to the

Fourier spectrum of the measured response. The auto-correlation function is then obtained from the inverse Fourier transform with a Hanning window and 50% overlapping. The obtained auto-correlation function is then used as the input to the improved HHT method for obtaining the instantaneous frequencies, which are shown in Figure 13. These results show that the improved HHT method can identify the low frequency components accurately. However, for the high frequency information, even with such narrow band-pass filters for signal pre-processing, the fluctuations are observed for the third and fourth frequencies and the relative errors are about 7%. The error may be caused by the pass band ripples in the band pass filter design. It should be noted that the end-effect and the associated errors in the modal identification are also observed at the end of the signals.

The proposed approach based on VMD is then applied to the same response signal. The identified IMFs and instantaneous frequencies are shown in Figures 14 and 15, respectively. The four identified frequencies of the steel structure are 5.17Hz, 15.05Hz, 23.52Hz, and 29.20Hz, respectively, which are the same as the modal identification results using DIAMOND [38]. It should be noted that the proposed approach can be used for both the time-invariant and time-varying systems, in this time-invariant case, it well separates and identifies the modal frequencies of a steel frame structure, and outperforms the existing HHT method with more reliable and steady modal identification results with less fluctuations. In the next section, experimental studies on the instantaneous frequency identification of a time-varying structure will be conducted.

#### **4.2 Instantaneous frequency identification of a time-varying structure**

The second example is a time-varying bridge-vehicle system as shown in Figure 16. The slab of the testing T-section prestressed concrete beam has a length of 5 m, a width of 0.65 m, and a total height of 0.415 m. The initial Young's modulus and density are 26.0 GPa and 2707.7 kg/m<sup>3</sup>, respectively. Experimental setup is shown in Figure 16(a) by using a motor to pull over the vehicle travelling on the testing beam. Three prestressing tendons with each of a cross section area of 99.8 mm<sup>2</sup> are included in the web with a total prestress force of 140 kN. The tendon's profile is parabolic and the locations at the ends and mid-span of the beam are shown in Figure 16(b). A vehicle model was designed and fabricated as shown in Figure 16(c). The spacing of the front and rear axles is 0.8 m and the lateral spacing of two wheels is 0.4 m. The

total weight of the model is 9.8kN. The vehicle was pulled by an electrical motor to run on the beam with an approximately constant speed of 0.4 m/s. Seven accelerometers were installed on the beam structure to measure the vibration responses under the moving vehicle. Approximately 13 seconds of response data were recorded when the vehicle was running on the beam, sampled at 1000Hz and filtered with a bandwidth frequency of 4–65 Hz. The fundamental natural frequency of the beam structure is 33.4 Hz without considering the effect of the moving vehicle. This bridge-vehicle system is time-varying because of the significant mass ratio between the vehicle and the bridge, as well as the changing excitation locations. The details of the experimental setup and test descriptions can be found in [39].

Figure 17 shows the measured response at the mid span of the beam along with its Fourier spectrum. It can be observed that most of the energy is distributed in the frequency range of 5-40Hz. The frequency corresponding to the maximum energy is around 33Hz, and significant vibrations occur within the frequency range from 20Hz-40Hz. The bridge vibration is dominated by the fundamental frequency of the bridge-vehicle system because the vehicle is crossing the bridge with a slow speed at 0.4m/s as mentioned above. However, the vibration characteristics of the system are varying with the locations of the moving vehicle on the bridge. Significant fluctuation and noise exist in the responses during the periods when the vehicle enters and leaves the bridge model. Therefore only 10 second vibration data with both the front and rear wheels of on the bridge model are selected for identification in this study.

Both the improved HHT method [37] as mentioned in Section 4.1 and the proposed approach are employed to identify the instantaneous frequencies of this time-varying system with the measured acceleration response at the mid-span. The identification results by using the improved HHT method and the proposed approach are shown in Figures 18 and 19, respectively. The theoretical instantaneous frequencies considering the moving vehicle travelling on the top of the bridge with the calibrated speed from optical sensors are also calculated with “freezing method” [36] based on the updated finite element model [39] of the bridge-vehicle system. The minimum value of the first frequency is 18.99Hz when the vehicle locates at the middle span of the beam. Figure 18 shows the identified instantaneous frequency from the first two IMFs with EMD. Two significant frequency components are identified and cannot be well separated. The real instantaneous frequency of the first vibration mode cannot be identified in this case.

By using VMD, a single frequency component is identified as shown in Figure 19. The Hilbert spectrum of the extracted IMF is shown in Figure 19(a). At the beginning and end of the signal, the instantaneous frequency is about 30Hz, while it is about 20Hz when the vehicle is in the middle of the bridge. It should be noted that instantaneous frequency identification of a bridge-vehicle system is challenging due to the low signal-to-noise ratio in the measured response signals from such a time-varying system with a slow moving speed and the non-negligible interaction from the moving vehicle [40]. Significant fluctuations in the identified instantaneous frequencies are observed because of the uncertainties of the bridge-vehicle interaction and the measurement noise. The polynomial curve fitting technique is therefore used to fit the identified results with the second order parabola. The obtained fitted curve is compared with the theoretical instantaneous frequencies, as shown in Figure 19(b). It is observed that the fitted curve matches with the theoretical value well, indicating the effectiveness and accuracy of the proposed approach in identifying the instantaneous frequency of a time-varying system with significant uncertainties and measurement noise.

## 5 Conclusions

Many methods, such as EMD, AMD and wavelet based techniques, have been proposed for signal decomposition. VMD is a novel method that decomposes a signal into an ensemble of band-limited IMFs. This paper proposes an approach for the instantaneous frequency identification of time-varying structures based on VMD and Hilbert transform. The measured response signal is decomposed into a finite number of IMFs with VMD, and then Hilbert transform is performed for the identification of instantaneous frequencies. Numerical studies on time-varying systems with smooth and periodical variations are conducted to investigate the accuracy and performance of the proposed approach. Finally experimental validations on a time-invariant steel frame structure and a time-varying bridge-vehicle system in the laboratory are carried out. Both numerical and experimental studies demonstrate that the proposed approach can well perform the signal decomposition with limited bandwidth of the individual modes and identify the instantaneous frequency of the time-varying systems accurately. It might be possible to obtain the time-varying mode shapes ~~varying with time~~, providing that a sufficient number of sensors have been deployed. The time-varying mode shape can be obtained based on the amplitudes at the resonant frequencies of each mode. The feasibility and

performance of using VMD for the identification of closely spaced modes will be explored in the future studies.

## Acknowledgements

The work described in this paper was supported by the National Research Foundation of Korea (NRF) grant funded by the Korea government (MSIP) through GCRC-SOP (No. 2011-0030013) and an ARC linkage project LP160100528.

## References

- [1] D.J. Ewins, Modal testing: theory, practice and application, 2<sup>nd</sup> Edition, Research Studies Press Ltd, England, 2003.
- [2] R. Brincker, L. Zhang, P. Andersen, Modal identification of output-only systems using frequency domain decomposition, *Smart Materials and Structures*, 10 (2001) 441.
- [3] B.H. Kim, N. Stubbs, T. Park, A new method to extract modal parameters using output-only responses, *Journal of Sound and Vibration*, 282 (2005) 215-230.
- [4] B. Peeters, G. De Roeck, Reference-based stochastic subspace identification for output-only modal analysis, *Mechanical Systems and Signal Processing*, 13 (1999) 855-878.
- [5] J.-N. Juang, R.S. Pappa, An eigensystem realization algorithm for modal parameter identification and model reduction, *Journal of Guidance, Control, and Dynamics*, 8 (1985) 620-627.
- [6] J.M. Caicedo, S.J. Dyke, E.A. Johnson, Natural excitation technique and eigensystem realization algorithm for phase I of the IASC-ASCE benchmark problem: Simulated data, *Journal of Engineering Mechanics*, 130 (2004) 49-60.
- [7] Q. Qin, H. Li, L. Qian, C.-K. Lau, Modal identification of Tsing Ma bridge by using improved eigensystem realization algorithm, *Journal of Sound and Vibration*, 247 (2001) 325-341.
- [8] M. Döhler, X.-B. Lam, L. Mevel, Uncertainty quantification for modal parameters from stochastic subspace identification on multi-setup measurements, *Mechanical Systems and Signal Processing*, 36 (2013) 562-581.
- [9] F.L. Zhang, Y.C. Ni, S.K. Au, H.F. Lam, Fast Bayesian approach for modal identification using free vibration data, Part I–Most probable value, *Mechanical Systems and Signal Processing*, 70 (2016) 209-220.
- [10] W.J. Yan, L.S. Katafygiotis, A novel Bayesian approach for structural model updating utilizing statistical modal information from multiple setups, *Structural Safety*, 52 (2015) 260-271.
- [11] W.J. Yan, L.S. Katafygiotis, A two-stage fast Bayesian spectral density approach for ambient modal analysis. Part I: posterior most probable value and uncertainty, *Mechanical Systems and Signal Processing*, 54 (2015) 139-155.
- [12] K.V. Yuen, J.L. Beck, Updating properties of nonlinear dynamical systems with uncertain input, *ASCE Journal of Engineering Mechanics*, 129 (2003) 9-20.
- [13] H.F. Lam, F.L. Zhang, Y.C. Ni, J. Hu, Operational modal identification of a boat-shaped



building by a Bayesian approach, *Engineering Structures*, 138 (2017) 381-393.

[14] S.K. Au, Y. Ni, F. Zhang, H. Lam, Full-scale dynamic testing and modal identification of a coupled floor slab system, *Engineering Structures*, 37 (2012) 167-178.

[15] W.-J. Yan, W.-X. Ren, An Enhanced Power Spectral Density Transmissibility (EPSDT) approach for operational modal analysis: theoretical and experimental investigation, *Engineering Structures*, 102 (2015) 108-119.

[16] Y. Xia, Y.L. Xu, Z.L. Wei, H.P. Zhu, X.Q. Zhou, Variation of structural vibration characteristics versus non-uniform temperature distribution, *Engineering Structures*, 33 (2011) 146-153.

[17] H. Sohn, M. Dzwonczyk, E.G. Straser, A.S. Kiremidjian, K.H. Law, T. Meng, An experimental study of temperature effect on modal parameters of the Alamosa Canyon Bridge, *Earthquake Engineering & Structural Dynamics*, 28 (1999) 879-897.

[18] L. Faravelli, C. Fuggini, F. Ubertini, Toward a hybrid control solution for cable dynamics: Theoretical prediction and experimental validation, *Structural Control and Health Monitoring*, 17 (2010) 386-403.

[19] Y. Bao, Z. Shi, J.L. Beck, H. Li, T.Y. Hou, Identification of time-varying cable tension forces based on adaptive sparse time-frequency analysis of cable vibrations, *Structural Control and Health Monitoring*, 24 (2017) e1889.

[20] M. Spiridonakos, S. Fassois, Parametric identification of a time-varying structure based on vector vibration response measurements, *Mechanical Systems and Signal Processing*, 23 (2009) 2029-2048.

[21] N.E. Huang, Z. Shen, S.R. Long, M.C. Wu, H.H. Shih, Q. Zheng, N.-C. Yen, C.C. Tung, H.H. Liu, The empirical mode decomposition and the Hilbert spectrum for nonlinear and non-stationary time series analysis, *Proceedings of the Royal Society of London A: Mathematical, Physical and Engineering Sciences*, The Royal Society, 1998, pp. 903-995.

[22] Z.Y. Shi, S.S. Law, Identification of linear time-varying dynamical systems using Hilbert transform and empirical mode decomposition method, *ASME Journal of Applied Mechanics*, 74 (2007) 223-230.

[23] Y. Yang, K. Chang, Extraction of bridge frequencies from the dynamic response of a passing vehicle enhanced by the EMD technique, *Journal of Sound and Vibration*, 322 (2009) 718-739.

[24] H. Li, X. Deng, H. Dai, Structural damage detection using the combination method of EMD and wavelet analysis, *Mechanical Systems and Signal Processing*, 21 (2007) 298-306.

[25] J. Li, H. Hao, Damage detection of shear connectors under moving loads with relative displacement measurements, *Mechanical Systems and Signal Processing*, 60 (2015) 124-150.

[26] M. Feldman, Time-varying vibration decomposition and analysis based on the Hilbert transform, *Journal of Sound and Vibration*, 295 (2006) 518-530.

[27] G. Chen, Z. Wang, A signal decomposition theorem with Hilbert transform and its application to narrowband time series with closely spaced frequency components, *Mechanical Systems and Signal Processing*, 28 (2012) 258-279.

[28] Z. Wang, G. Chen, Analytical mode decomposition with Hilbert transform for modal parameter identification of buildings under ambient vibration, *Engineering Structures*, 59 (2014) 173-184.

[29] Z.-C. Wang, G.-D. Chen, Analytical mode decomposition of time series with decaying

amplitudes and overlapping instantaneous frequencies, *Smart Materials and Structures*, 22 (2013) 095003.

[30] C. Wang, W.X. Ren, Z.C. Wang, H.P. Zhu, Instantaneous frequency identification of time-varying structures by continuous wavelet transform, *Engineering Structures*, 52 (2013) 17-25.

[31] W.J. Staszewski, D.M. Wallace, Wavelet-based Frequency Response Function for time-variant systems—An exploratory study, *Mechanical Systems and Signal Processing*, 47 (2014) 35-49.

[32] K. Dragomiretskiy, D. Zosso, Variational mode decomposition, *IEEE Transactions on Signal Processing*, 62 (2014) 531-544.

[33] Y.-J. Xue, J.-X. Cao, D.-X. Wang, H.-K. Du, Y. Yao, Application of the Variational-Mode Decomposition for Seismic Time-frequency Analysis. *IEEE Journal of Selected Topics in Applied Earth Observations and Remote Sensing*, 9(2016), 3821-3831.

[34] Y. Liu, G. Yang, M. Li, H. Yin, Variational mode decomposition denoising combined the detrended fluctuation analysis, *Signal Processing*, 125 (2016) 349-364.

[35] S. Boyd, N. Parikh, E. Chu, B. Peleato, J. Eckstein, Distributed optimization and statistical learning via the alternating direction method of multipliers, *Foundations and Trends® in Machine Learning*, 3 (2011) 1-122.

[36] J. Cooper, Identification of time varying modal parameters, *Aeronautical Journal*, 94 (1990) 271-278.

[37] C. Bao, H. Hao, Z.-X. Li, X. Zhu, Time-varying system identification using a newly improved HHT algorithm, *Computers & Structures*, 87 (2009) 1611-1623.

[38] S.W. Doebling, C.R. Farrar, P.J. Cornwell, DIAMOND: A graphical interface toolbox for comparative modal analysis and damage identification, *Proceedings of the 6th International Conference on Recent Advances in Structural Dynamics*, Southampton, UK, 1997, pp. 399-412.

[39] J. Li, S. Law, H. Hao, Improved damage identification in bridge structures subject to moving loads: numerical and experimental studies, *International Journal of Mechanical Sciences*, 74 (2013) 99-111.

[40] S. Marchesiello, S. Bedaoui, L. Garibaldi, P. Argoul, Time-dependent identification of a bridge-like structure with crossing loads, *Mechanical Systems and Signal Processing*, 23 (2009) 2019-2028.

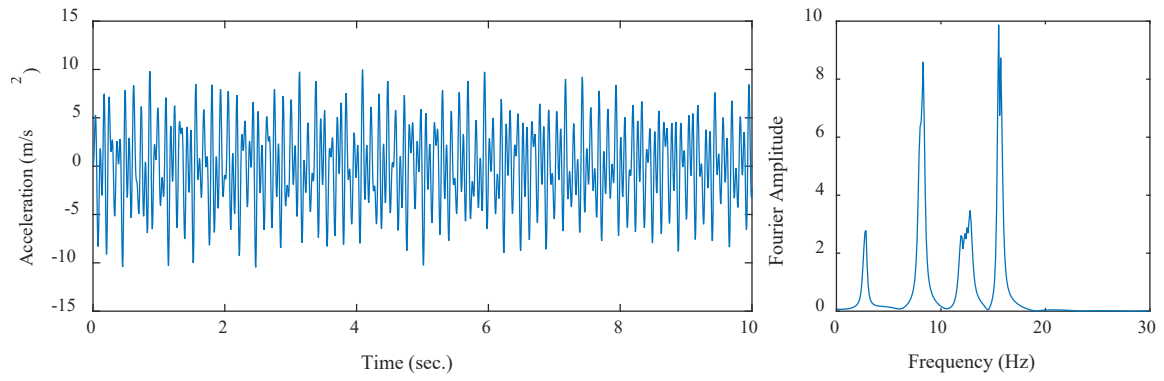


Figure 1. Time domain response signal and its fast Fourier transform spectrum in the numerical study (Case 1)

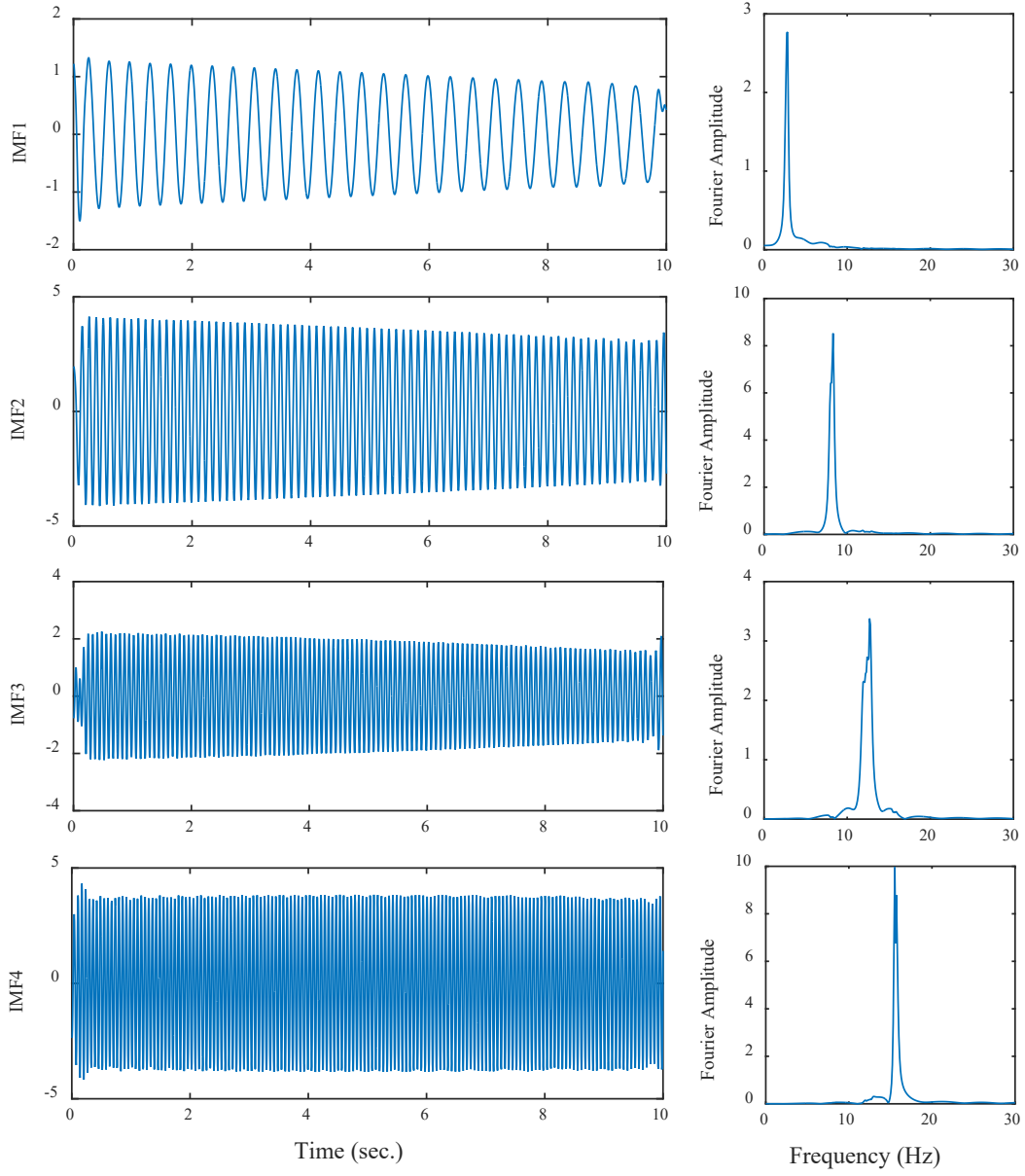


Figure 2. Decomposed IMFs of the response signal with VMD in the numerical study  
(Case 1)

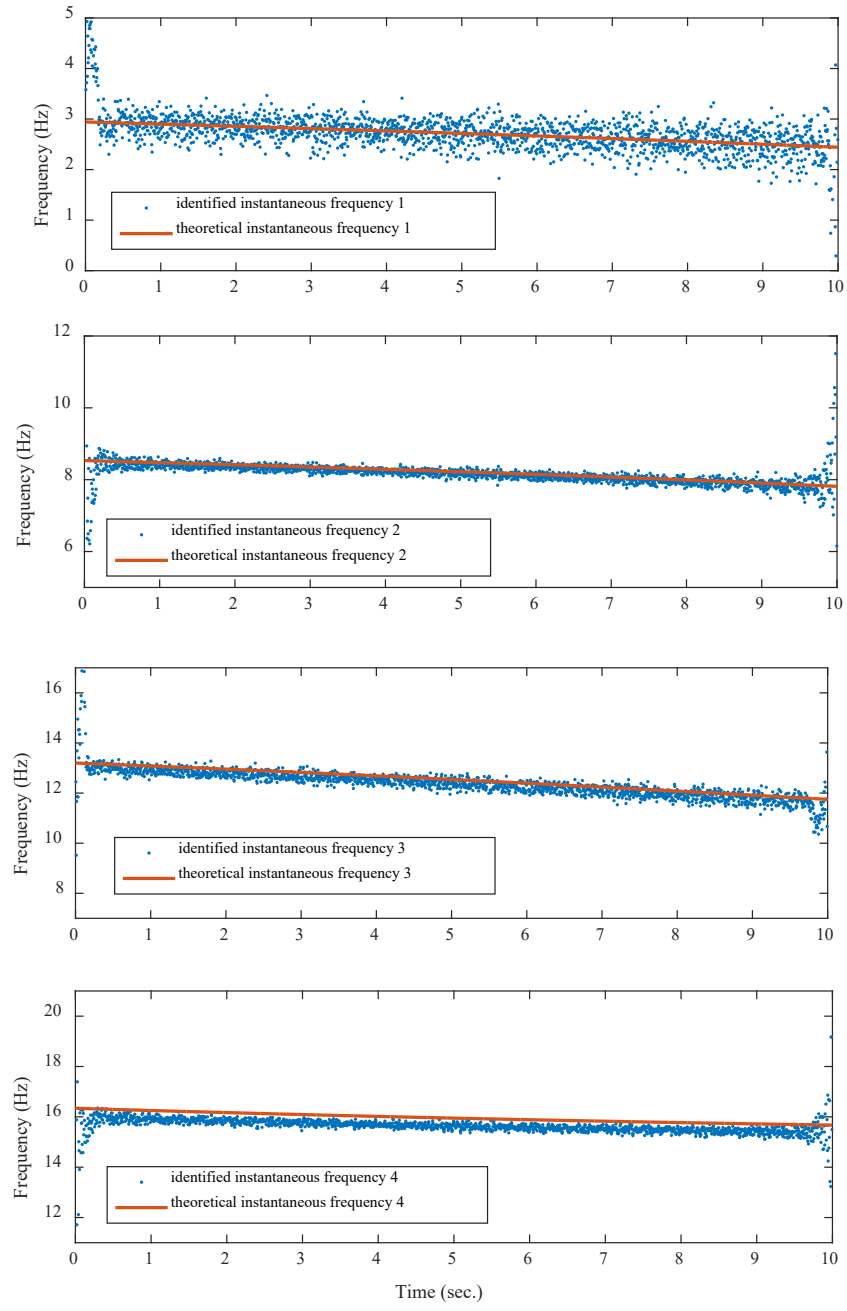


Figure 3. Identified instantaneous frequencies with VMD in the numerical study (Case 1)

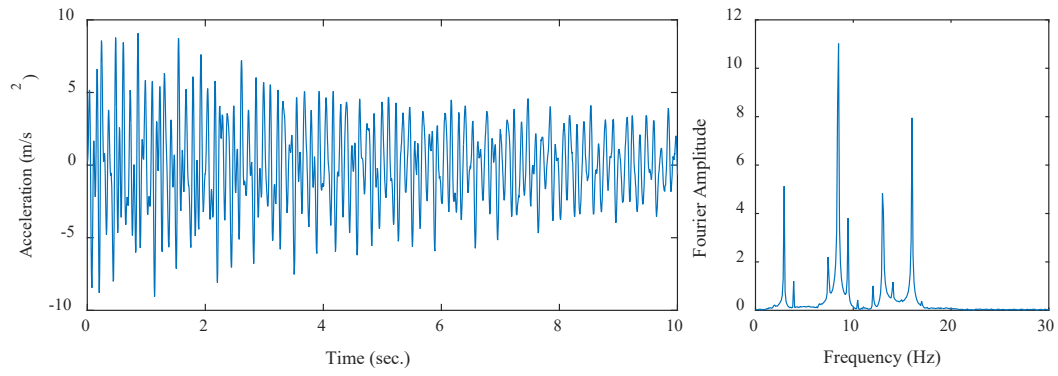


Figure 4. Time domain response signal and its fast Fourier transform spectrum in the numerical study (Case 2)

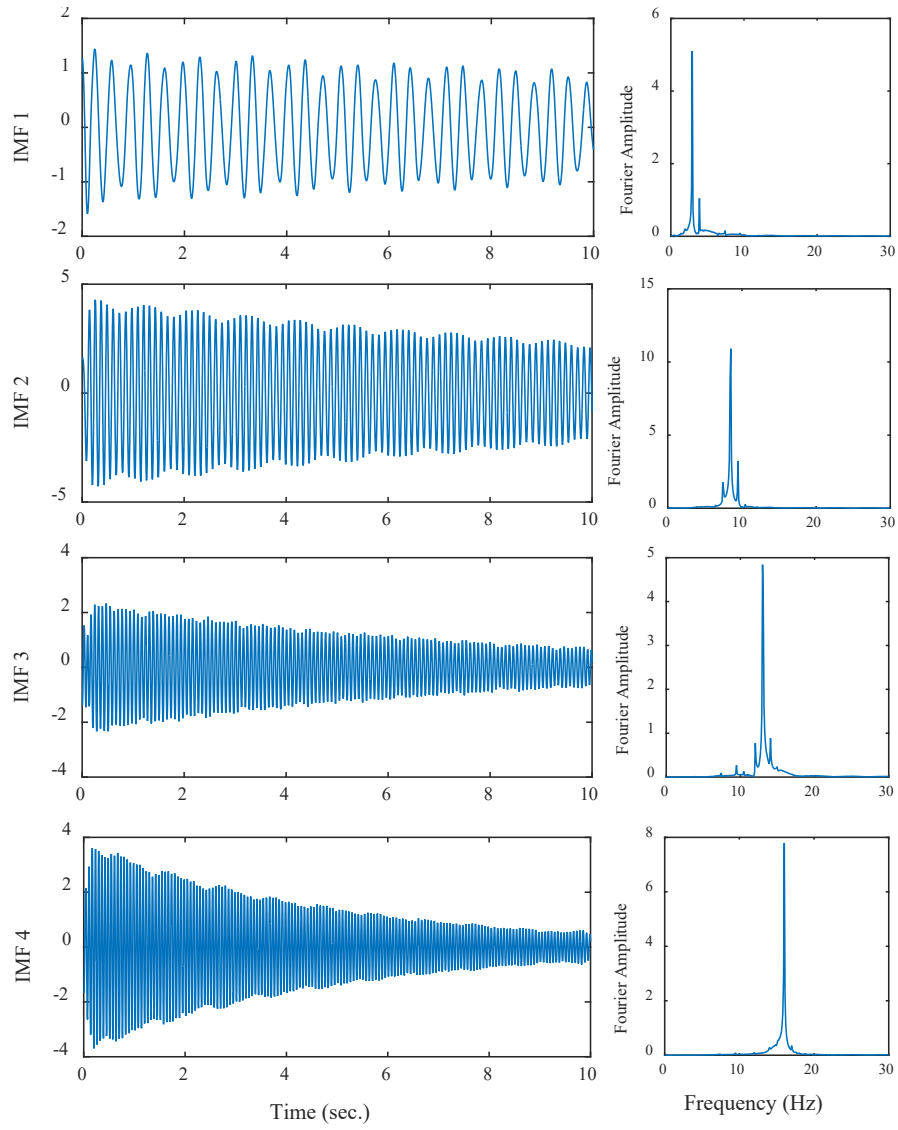


Figure 5. Decomposed IMFs of the response signal with VMD in the numerical study  
(Case 2)

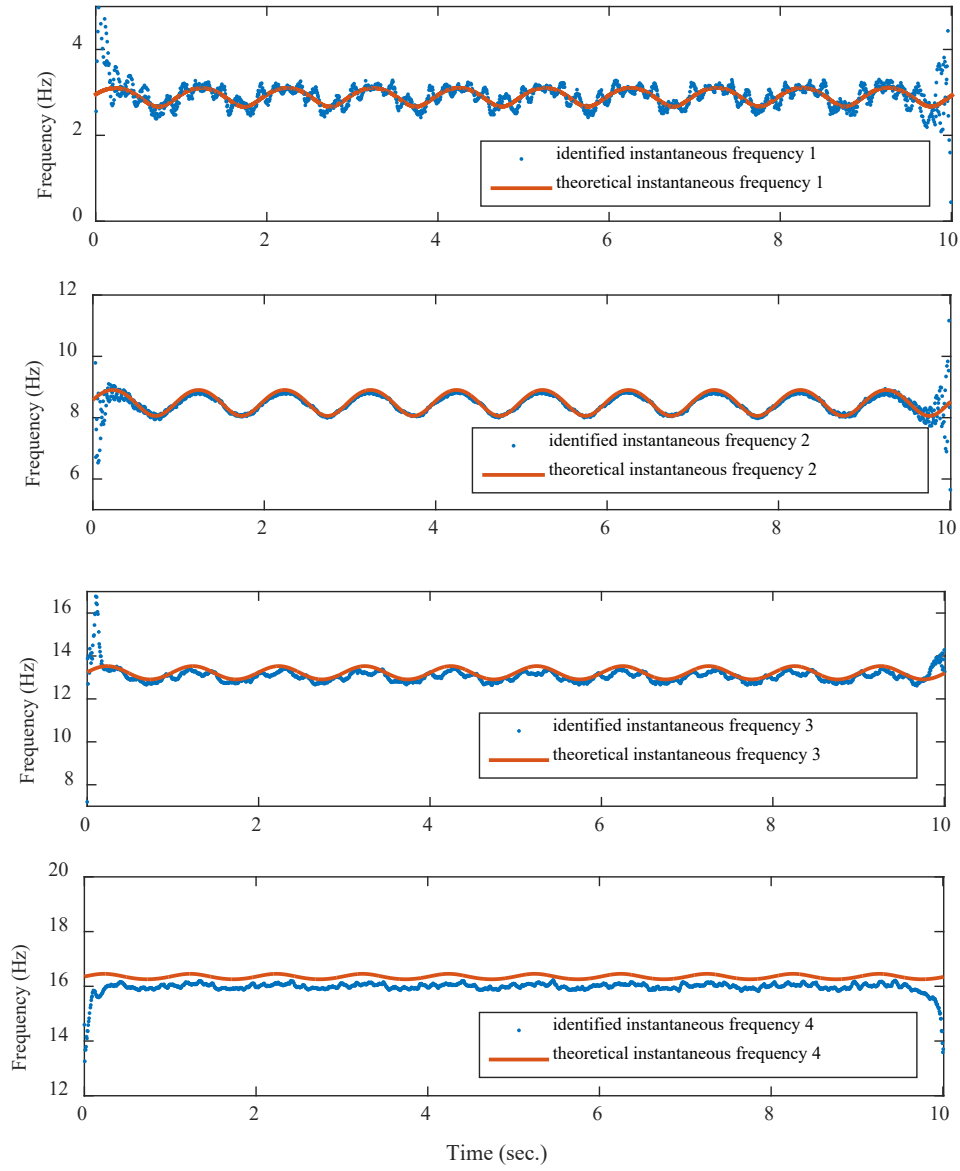


Figure 6. Identified instantaneous frequencies with VMD in the numerical study (Case 2)



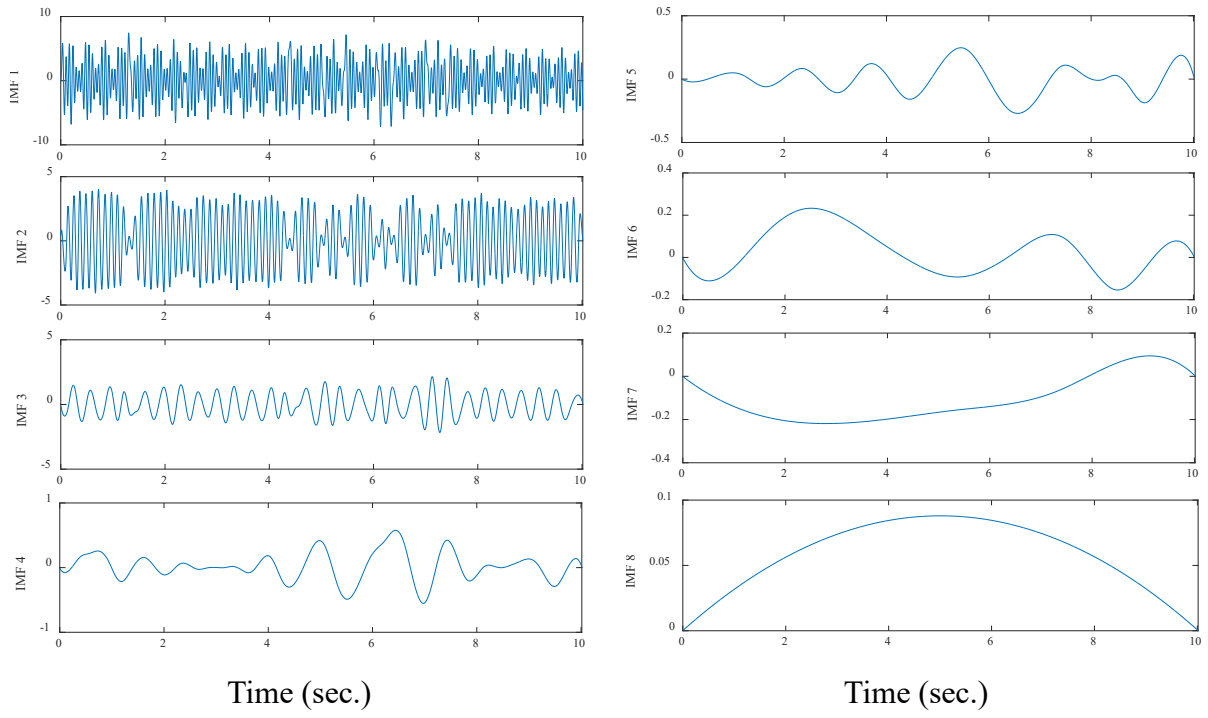
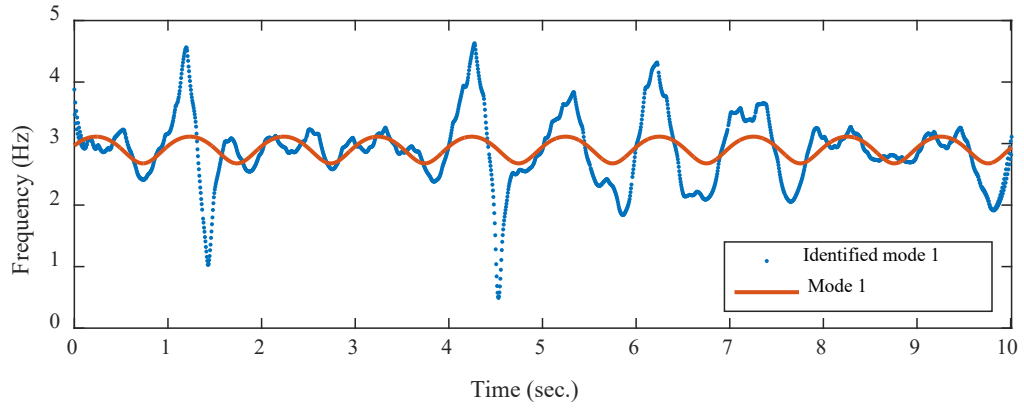
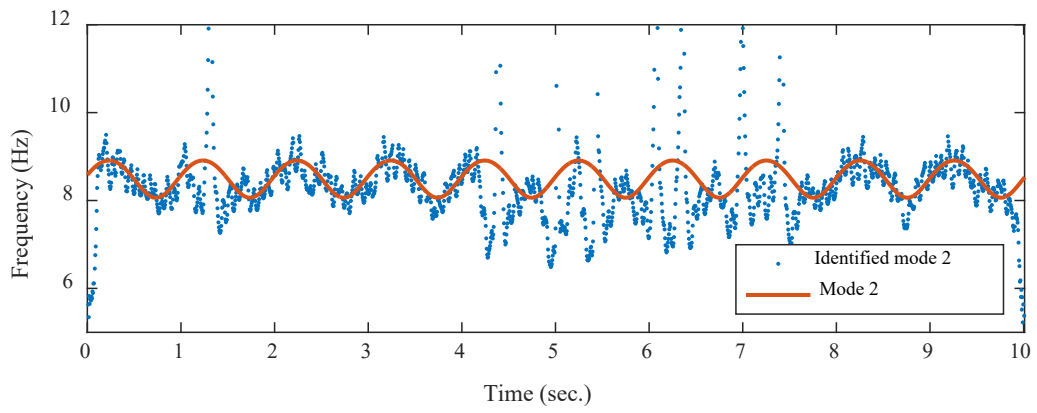


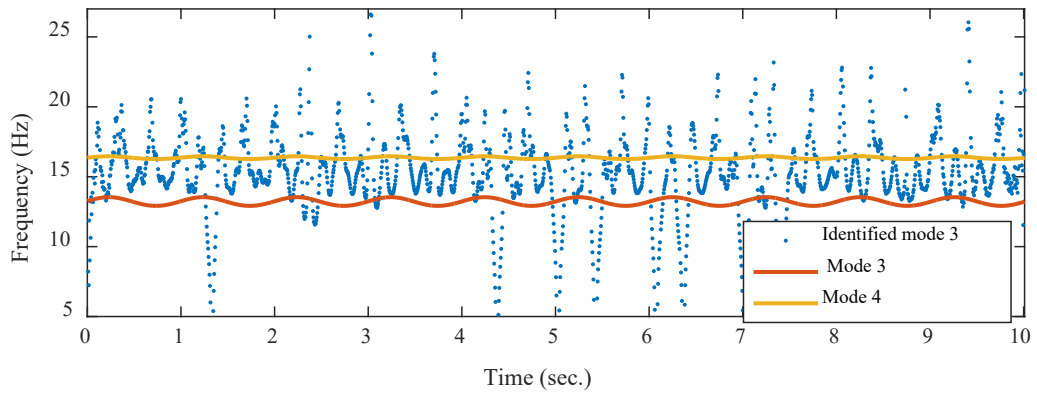
Figure 7. Extracted IMFs of the response signal with EMD in the numerical study  
(Case 2)



(a) Identified instanetance frequency from IMF 1

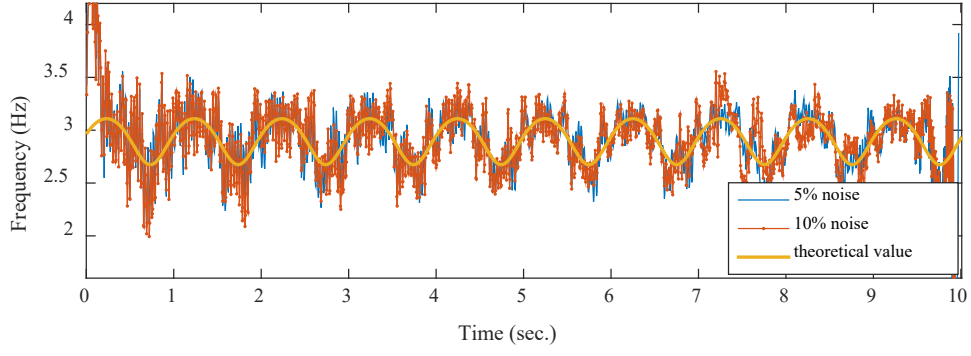


(b) Identified instanetance frequency of IMF 2

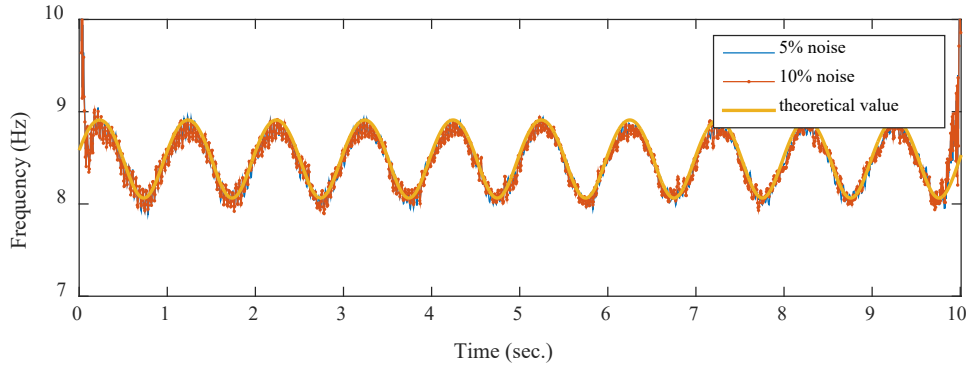


(c) Identified instanetance frequency of IMF 3

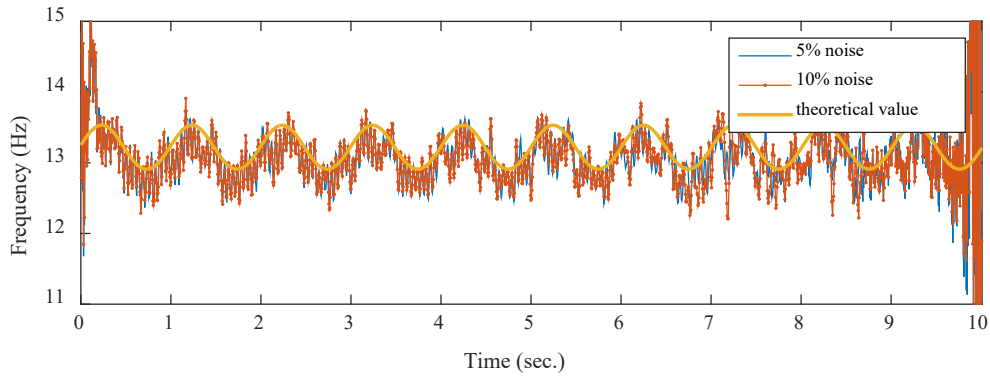
Figure 8. Identified instantaneous frequencies with EMD in the numerical study (Case 2)



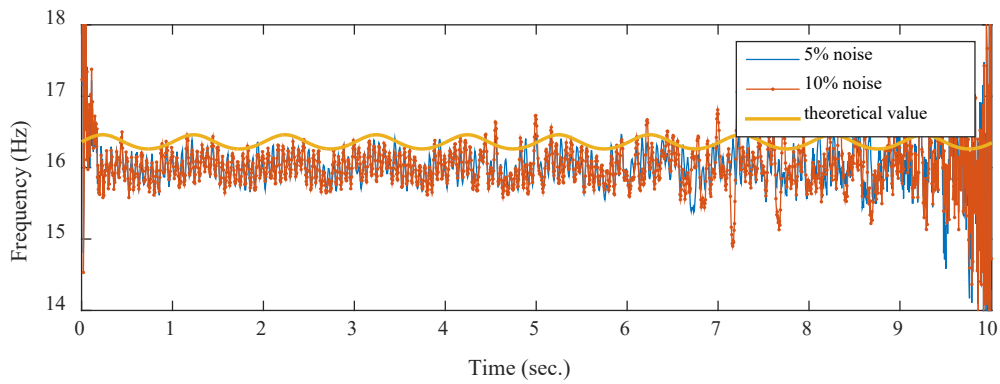
(a) Identified instantaneous frequency of mode 1



(b) Identified instantaneous frequency of mode 2



(c) Identified instantaneous frequency of mode 3



(d) Identified instantaneous frequency of mode 4

Figure 9. Identified instantaneous frequencies with VMD under different noise levels in the numerical study (Case 2)

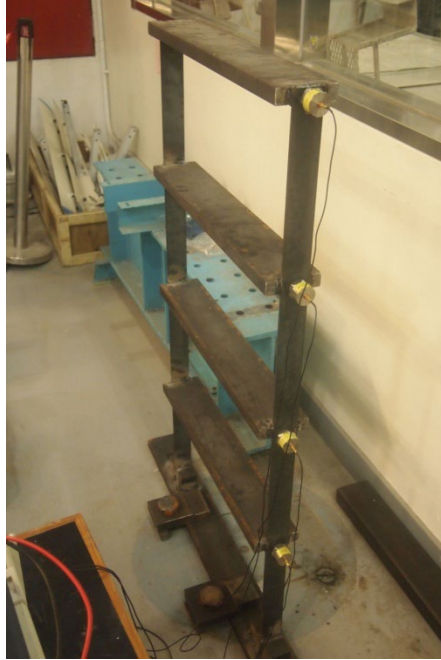
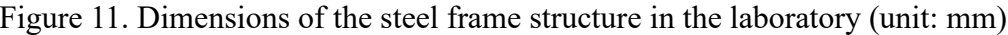
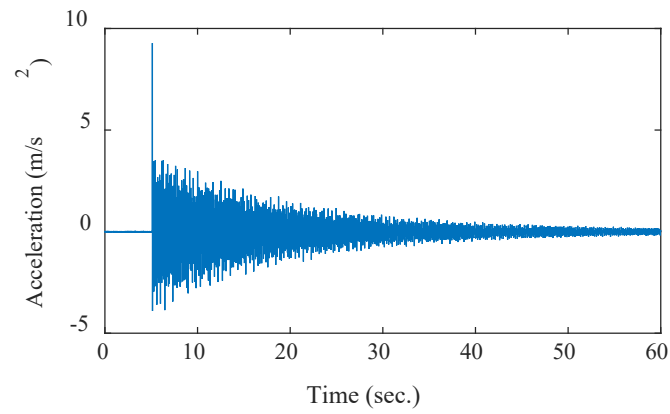
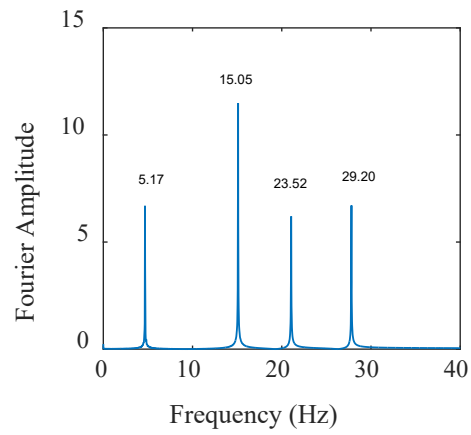


Figure 10. A steel frame model in the laboratory





(a) Time history of measured response at the top floor



(b) Fourier spectrum of measured response at the top floor

Figure 12. Measured acceleration response at the top floor of the frame and its fast Fourier transform spectrum under a hammer excitation

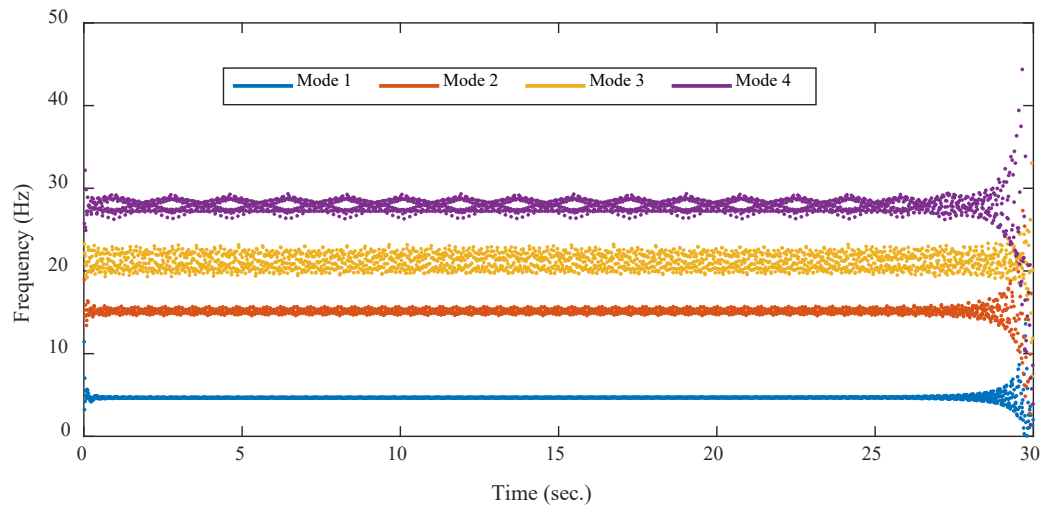


Figure 13. Identified instantaneous frequencies from an improved HHT method in the experimental study

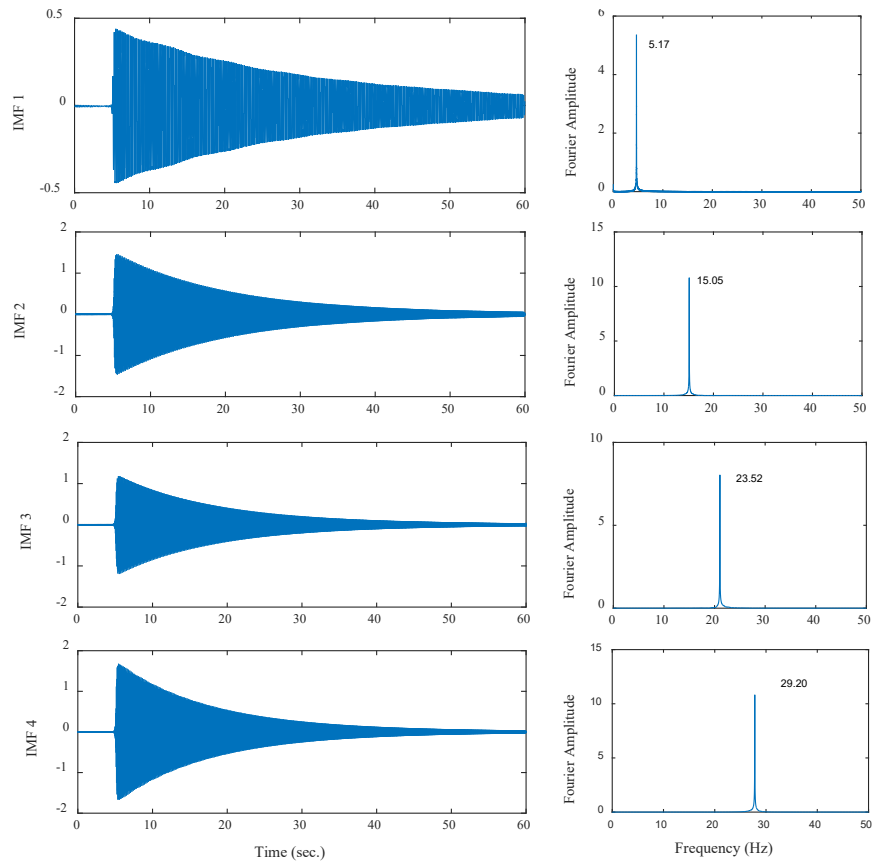


Figure 14. Identified IMFs with VMD in the experimental study



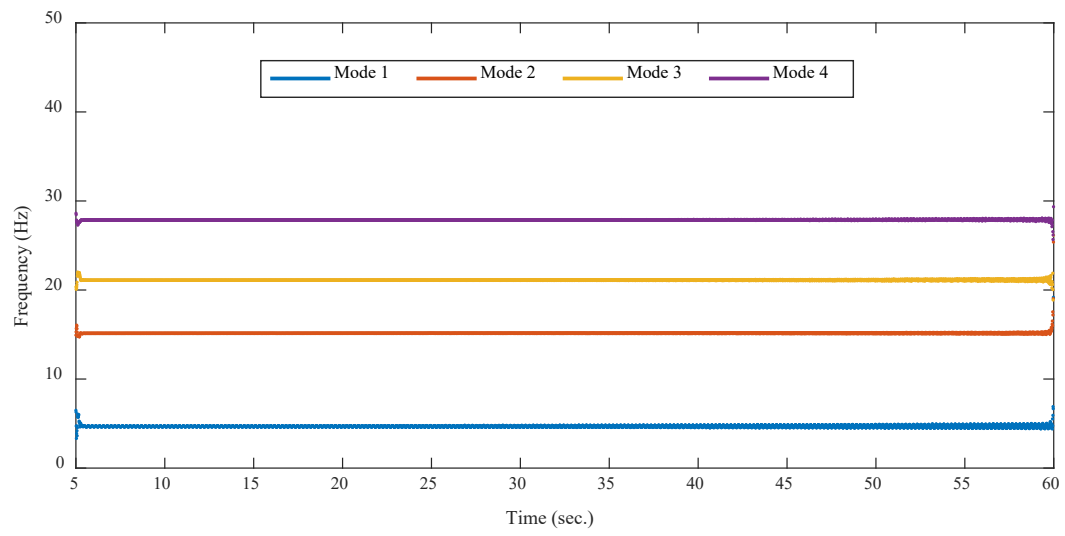
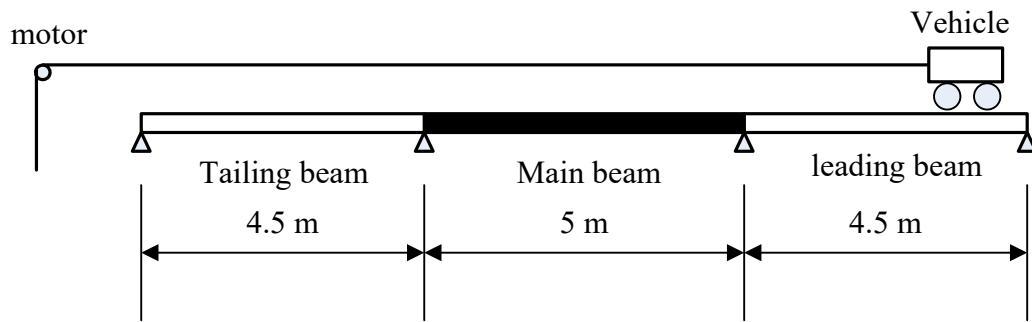
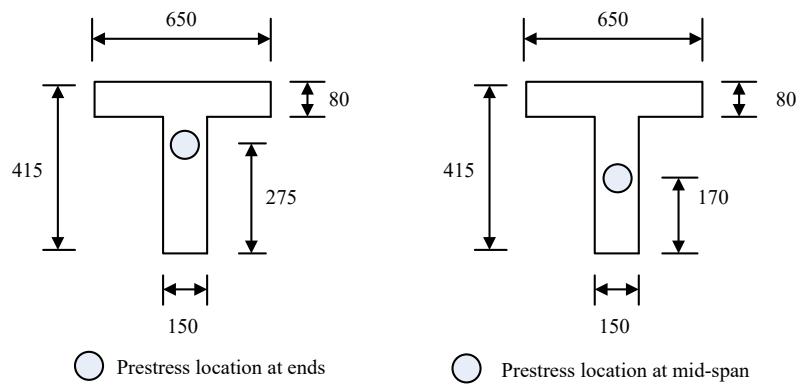


Figure 15. Identified instantaneous frequencies with VMD



(a) Schematic experimental setup



(b) Cross section of T-beam



(c) Overview of the experiment setup and vehicle model

Figure 16. Experimental setup of a bridge-vehicle system in the laboratory

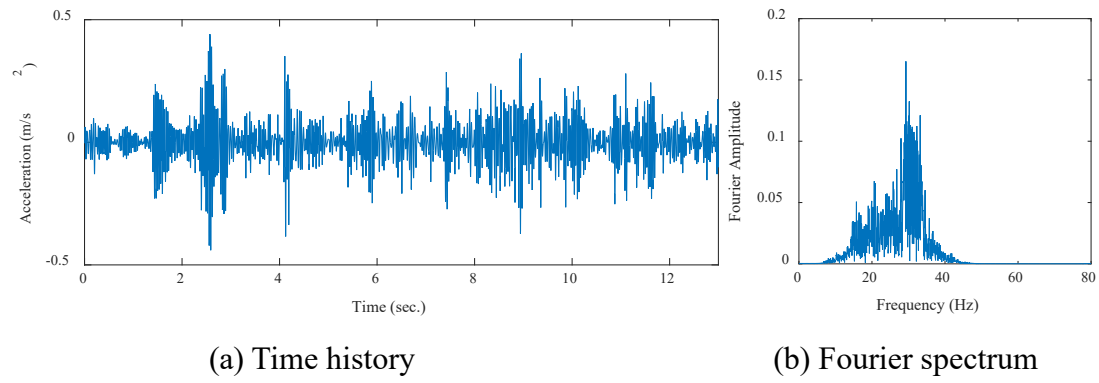


Figure 17. Time history and fast Fourier transform spectrum of the measured response at the middle span of the beam

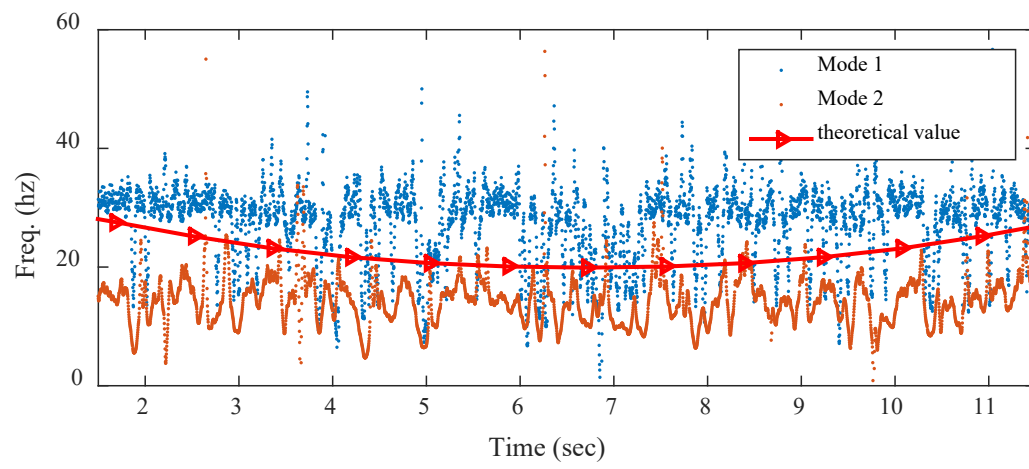
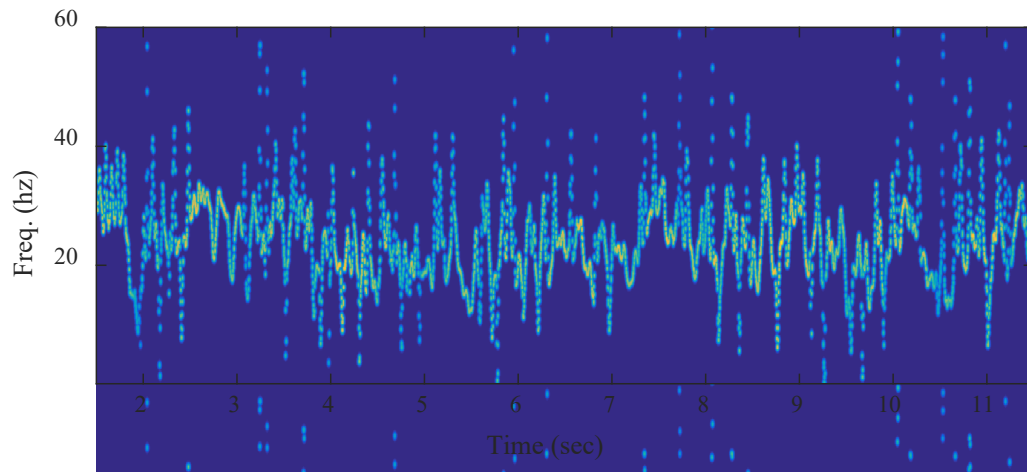
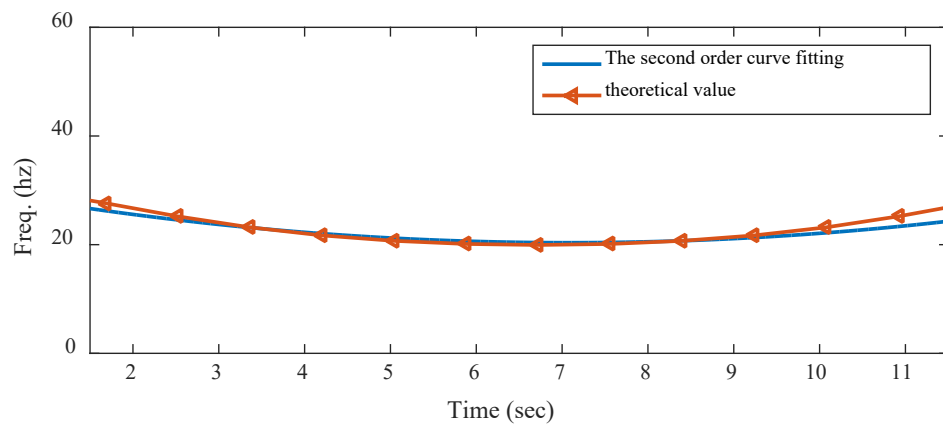


Figure 18. Identified instantaneous frequencies of the bridge-vehicle system with EMD



(a) Hilbert spectrum



(b) Identified instantaneous frequencies and therotical value

Figure 19. Identified instantaneous frequencies of the bridge-vehicle system with VMD